In-beam γ-ray spectroscopy of the neutron-rich nitrogen isotopes $^{19-22}$N

D. Sohler,[1] M. Stanoiu,[2,3] Zs. Dombrádi,[1] F. Azaiez,[2] B. A. Brown,[4] M. G. Saint-Laurent,[3] O. Sorlin,[3] Yu.-E. Penionzhkevich,[5] N. L. Achouri,[6] J. C. Angélique,[6] M. Belleguic,[2] C. Borcea,[7] C. Bourgeois,[2] J. M. Daugas,[3] F. De Oliveira-Santos,[3] Z. Dlouhy,[8] C. Donzaud,[2] J. Duprat,[2] Z. Elekes,[1] S. Grévy,[3] D. Guillemaud-Mueller,[2] F. Ibrahim,[2] S. Leenhardt,[2] M. Lewitowicz,[3] M. J. Lopez-Jimenez,[3] S. M. Lukyanov,[5] W. Mittig,[3] J. Mrázek,[8] F. Negoita,[7] Zs. Podolyák,[9] M. G. Porquet,[10] F. Pougheon,[2] P. Roussel-Chomaz,[3] H. Savajols,[3] G. Sletten,[11] Y. Sobolev,[5] C. Stodel,[3] and J. Timár[1]

[1]*Institute of Nuclear Research of the Hungarian Academy of Sciences, P. O. Box 51, Debrecen, H-4001, Hungary*
[2]*Institut de Physique Nucléaire, IN2P3-CNRS, F-91406 Orsay Cedex, France*
[3]*GANIL, B. P. 55027, F-14076 Caen Cedex 5, France*
[4]*National Superconducting Cyclotron Laboratory, Michigan State University, East Lansing, Michigan 48824, USA*
[5]*FLNR, JINR, RU-141980 Dubna, Moscow region, Russia*
[6]*Laboratoire de Physique Corpusculaire, 6, bd du Mal Juin, F-14050 Caen Cedex, France*
[7]*IFIN-HH, P. O. Box MG-6, RO-76900 Bucharest-Magurele, Romania*
[8]*Nuclear Physics Institute, AS CR, CZ 25068, Rez, Czech Republic*
[9]*Department of Physics, University of Surrey, Guildford, GU2 7XH, United Kingdom*
[10]*CSNSM, IN2P3-CNRS and Université Paris-Sud, F-91405 Orsay Campus, France*
[11]*Niels Bohr Institute, Blegdamsvej 17, DK-2100, Copenhagen, Denmark*

(Received 30 May 2007; published 9 April 2008)

The structure of $^{19-22}$N nuclei was investigated by means of in-beam γ-ray spectroscopic technique using fragmentation reactions of both stable and radioactive beams. Based on particle-γ and particle-$\gamma\gamma$ coincidence data, level schemes are constructed for the neutron-rich nitrogen nuclei. The experimental results are compared with shell model calculations. The strength of the $N = 14$ and $Z = 8$ shell closures and the weakening of the shell model interaction WBT are discussed.

DOI: 10.1103/PhysRevC.77.044303 PACS number(s): 23.20.Lv, 21.60.Cs, 27.30.+t, 25.70.Mn

I. INTRODUCTION

In the last 20 years, significant experimental and theoretical efforts have been devoted to the investigation of the shell structure of light neutron-rich nuclei close to the drip line. Recently, it has been shown that the proton p shell nuclei with 2–3 valence neutrons above the $N = 8$ shell closure have a weaker neutron-neutron effective interaction than expected. More precisely, the USD part of the WBT interaction of Warburton and Brown [1] needs to be reduced to describe the excitation energies of the neutron-rich carbon and boron nuclei [2,3]. Similar differences between theory and experiment were observed concerning the excited states of ^{17}N, as well as the magnetic moment of the odd boron isotopes [4]. In the present paper, we extend the systematics by new experimental data on $^{19-22}$N, and investigate the strength of the effective interaction next to the $Z = 8$ region. Special emphasis is placed on the strength of the $N = 14$ subshell closure which seems to disappear in the $Z = 6$ nucleus ^{20}C [3].

Recently, the weakening of the $Z = 8$ shell closure has also been reported in ^{20}O [5] observed by study of the proton cross shell excitations which are known in the nitrogen isotopes, as well. The extension of their investigations into a more neutron-rich region might provide information on the strength of the $Z = 8$ shell closure up to $N = 14$ at $Z = 7$.

Previously, limited knowledge on the excited states of ^{19}N was collected from multinucleon transfer reactions [6,7]. From these, it is expected that the states arising from a coupling of the $p_{1/2}$ proton hole to the 2^+, 4^+ states of the ^{20}O core are mostly excited [7]. The ground state spin of ^{19,21}N was determined to be $1/2^-$ and that of ^{20}N to be 2^- [8]. No experimental data are available for the excited states of nitrogen nuclei heavier than $A = 19$.

II. EXPERIMENTAL METHOD

The experimental study of the heavy nitrogen isotopes was performed at GANIL by using the same methods which were already applied to investigate the neutron-rich oxygen [9] and neon [10] isotopes. Two experiments were carried out: the single-step and the double-step fragmentation reactions. In the first experiment, a ^{9}Be target of 2.77 mg/cm^2 thickness was bombarded by a $^{36}S^{16+}$ beam of 77.5 MeV A energy and of 1 pnA intensity. The emerging fragments were identified at the focal plane of GANIL's magnetic spectrometer (SPEG) by ionization and drift chambers, and a plastic scintillator determining their energy loss, position, total energy, and time of flight. The time data were corrected, to obtain a better resolution, by use of the position of the fragments in the focal plane of the SPEG. As we did not observe any overlap between the different charge states, this identification method alone gave a perfect separation of the fragments. The SPEG was tuned to the $A/Z = 8/3$ mass-to-charge ratio corresponding to about ^{19}N, but the isotope ^{21}N was also transmitted. In the experiment, about 2×10^6 ^{19}N, 1.5×10^5 ^{20}N, and 7500 ^{21}N nuclei were observed.

In the second experiment, we used a primary beam of ^{36}S delivered by the two GANIL cyclotrons at an energy of 77.5 MeV A and an intensity of 400 pnA on a carbon target

of 348 mg/cm^2 thickness placed in the SISSI device. The produced nuclei were selected through the ALPHA spectrometer using a 130 mg/cm^2 Al wedge. The magnetic rigidity of the ALPHA spectrometer and the optics of the beamline were optimized for the transmission of a secondary beam mainly composed of ^{24}F, ^{25,26}Ne, ^{27,28}Na, and ^{29,30}Mg fragments with energies varying from 54 to 65 MeV A. An "active" target composed of a plastic scintillator (103 mg/cm^2) sandwiched between two carbon foils of 51 mg/cm^2 each was used at the dispersive focus of the SPEG. The plastic scintillator part of the active target was used to identify the incoming nuclei via energy loss and time-of-flight measurements. The fragments induced by reactions of the secondary beam were collected and identified at the focal plane of the SPEG spectrometer, which was optimized for products with $A/Z = 3$. In this experiment, 16×10^3 ^{20}N, 9×10^3 ^{21}N, and 525 ^{22}N nuclei were observed.

The nitrogen nuclei produced in excited states in the fragmentation reactions decayed emitting γ rays in flight. These γ rays were observed by the "Chateau de crystal" BaF_2 array in both the single- and double-step fragmentation experiments. The 74 BaF_2 crystals of the Chateau were situated symmetrically above and below the target at a mean distance of 20 cm covering nearly 4π solid angle. The BaF_2 array had a photo-peak efficiency of about 30% at about 1.3 MeV with an average full width at half maximum (FWHM) of 12% after Doppler-correction. Because the crystals were closely packed, the γ rays could easily scatter among them. To decrease the background caused by the scattered γ rays, we used the array in add-back mode. In the single-step fragmentation experiment, four hyper pure Ge detectors were also placed around the target. The high-resolution Ge detectors of 70% efficiency were located at about 15 cm from the target at the most backward angles of 162° and 145° with respect to the beam direction. Their overall total photo-peak efficiency was ~0.12% at about 1.3 MeV. The Doppler shift caused by the large fragment velocity ($v/c = 0.34$) was taken into account as a correction in the γ-ray spectra. The additional information provided by the SPEG on the momenta of the fragments was also applied to improve the Doppler correction. After these corrections, a FWHM of about 38 keV was obtained at the γ-ray energy of ~1500 keV.

The high-resolution spectra of the Ge detectors helped to unfold the γ lines in the complex spectrum of ^{19}N and to precisely determine the energy of the most intense transition of ^{20,21}N. For the less populated heavier nitrogen isotopes, the weaker γ rays were identified by the BaF_2 detectors. The relatively high efficiency of this array made the observation of the $\gamma\gamma$-coincidence relations of the stronger transitions also possible, which were used to construct the level schemes.

III. EXPERIMENTAL RESULTS

The produced number of ^{19}N was large enough to have reasonable statistics in the γ-ray spectrum of the germanium detectors presented in Fig. 1. Besides the strongest 532 and 1141 keV transitions, several weaker γ lines appear. Therefore, we assign five additional γ rays with the energies of 1368, 1494, 1681, 2132, and 2347 keV to this nucleus. Furthermore, tentative γ lines at 2016 and 2507 keV are found with a 2.6σ confidence level.

Using the statistics obtained from the BaF_2 detectors, we could create also $\gamma\gamma$-coincidence matrices for ^{19}N. The $\gamma\gamma$-coincidence spectra gated on the most intense 532 and 1141 keV γ rays are shown in the insets of Fig. 1. From the analysis of the coincidence spectra, the 532, 1141, and 1494 keV transitions were found in mutual coincidences. The 532 and the 1141 keV γ rays seem to have coincidence

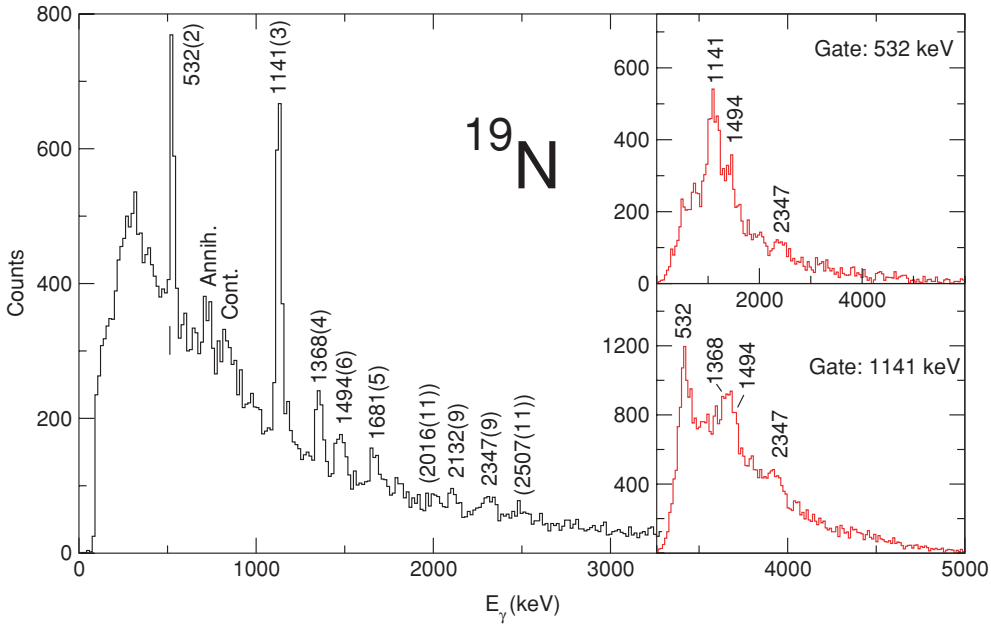

FIG. 1. (Color online) Ge γ-ray spectrum of ^{19}N obtained using the fragmentation of a ^{36}S beam on a ^{9}Be target. The insets present $\gamma\gamma$-coincidence spectra gated on the 532 and 1141 keV transitions analyzing the data collected by BaF_2 detectors.

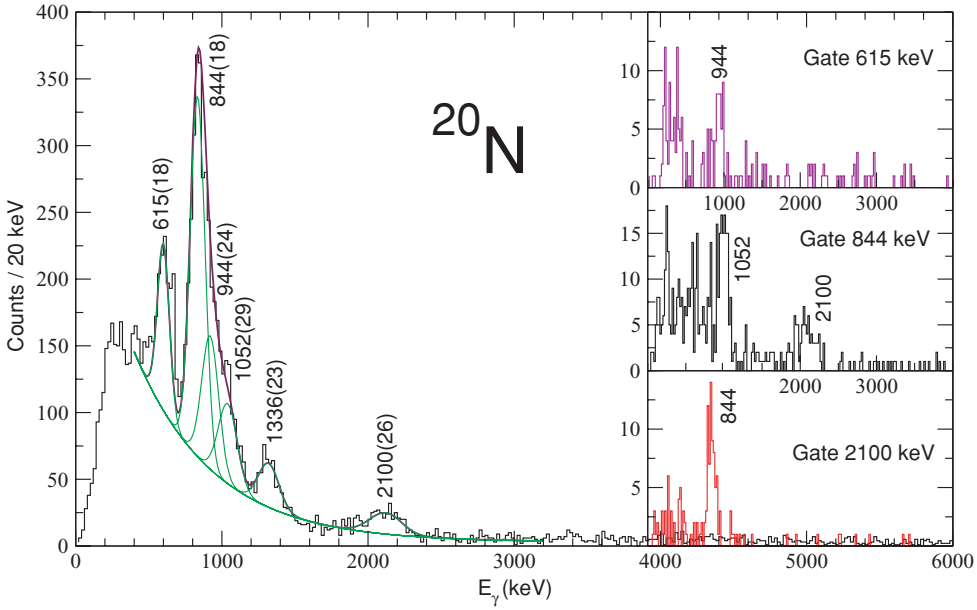

FIG. 2. (Color online) BaF_2 γ-ray spectrum of ^{20}N obtained in the double-step fragmentation reaction. The insets show BaF_2 coincidence spectra using the 615, 844, and 2100 keV transitions as gates.

relations also with the 2347 keV transition. In addition, the 1141 keV γ line is in coincidence with the 1368 keV transition, too. Although the 1368 and the 1494 keV γ rays could not be resolved in the projection spectrum of the coincidence matrix, by putting a gate on both of them, we could determine that one or both of them are in coincidence with the 1681 keV transition.

The heavier ^{20,21}N isotopes were produced by both the single- and double-step reactions. In the single-step reaction, the detectors were strongly overloaded by γ rays from other reaction channels, which resulted in a high background [10] as it is seen also in the coincidence spectra of ^{19}N shown in Fig. 1. The much cleaner conditions achieved in the radioactive beam experiment [9] resulted in a lower background, allowing the study of weaker radiations, too. Thus, in the following we mainly rely on the fragmentation of the radioactive beam.

In the BaF_2 spectrum of ^{20}N, four well-separated peaks are visible at 615(18), 844(18), 1336(23), and 2100(26) keV as shown in Fig. 2. The largest peak at 844 keV has a long tail, which is due to at least one overlapping peak. The $\gamma\gamma$-coincidence spectra presented in Fig. 2 show that the centroids of the peaks in the 800–1100 keV region seen in different gate spectra are different, and they suggest that the strongest peak is a triplet of γ rays with energies of 844, 944, and 1052 keV. The strongest 844 keV γ line is in coincidence with the 1052 and the 2100 keV ones, while the 615 keV line is in coincidence with the 944 keV one.

In the ^{20}N spectrum of the germanium detectors measured in the single-step fragmentation, only the 843(4) keV line is visible (Fig. 3), which makes possible a precise determination of its energy. In spite of the higher background, the existence of the 615, 843, 944, and 1336 keV transitions is confirmed by the BaF_2 spectrum of this reaction, too.

For ^{21}N, only the BaF_2 spectrum obtained in the double-step fragmentation (Fig. 4) has statistics large enough for transition assignment. A considerably wide peak at about 1180 keV dominates the spectrum. By determining the energy dependence of the peak width from the systematics of single peaks of other nuclei observed in the present experiment, this peak could be resolved into two γ rays with energies of 1159 and 1228 keV. In addition, we have a wide bump ranging from about 1600 to 2800 keV. This bump can be fitted by three weaker γ rays of 1790, 2142, and 2438 keV. Putting a wide gate on the 1159+1228 keV doublet, all the γ rays assigned to this nucleus are enhanced relative to the background; even the small peak at 884 keV becomes significant as shown in the inset of Fig. 4. Putting a narrow gate on the peaks in the wider bump, the 1790 keV transition is seen in coincidence with both the 1159 and 1228 keV γ rays, whereas the higher energy transitions see only the 1159 keV transition illustrated in the inset of Fig. 4 for the 2142 keV γ ray.

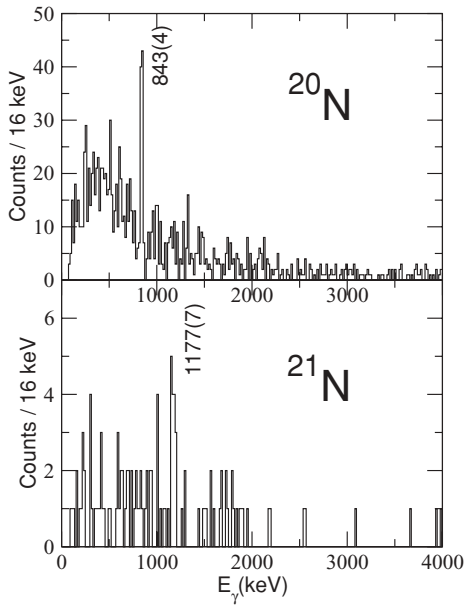

FIG. 3. Germanium γ-ray spectra of ^{20,21}N obtained in the single-step fragmentation reaction.

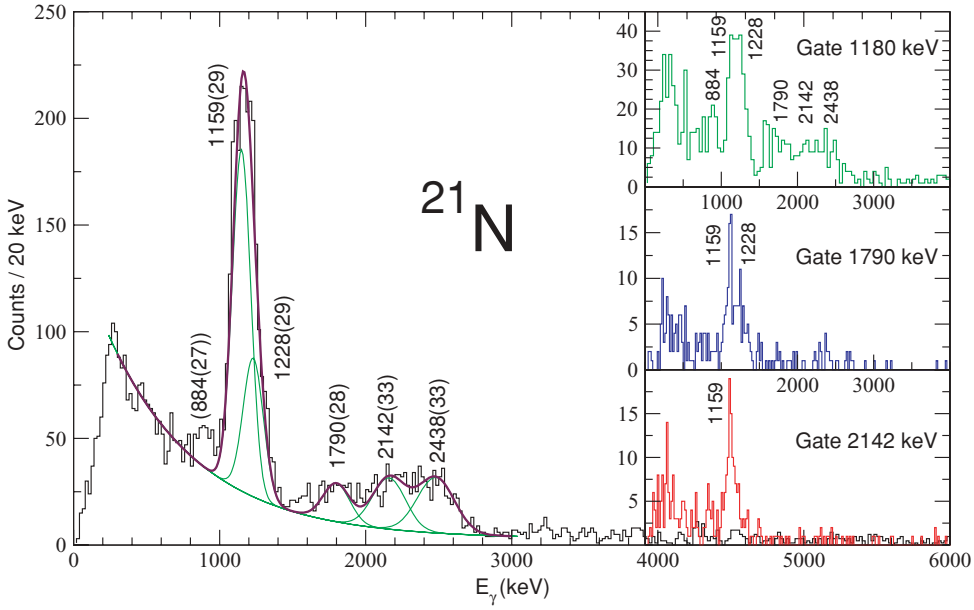

FIG. 4. (Color online) BaF_2 γ-ray spectrum of ^{21}N obtained in the double-step fragmentation reaction. The insets show BaF_2 coincidence spectra using the 1159+1228, 1790, and 2142 keV transitions as gates.

In the single-step reaction, the spectrum of the germanium detectors for ^{21}N shown in Fig. 3 contains only the strongest peak (the lower energy member of the intense doublet) resulting in its precise energy determination of 1177(7) keV. In the BaF_2 spectrum of the single-step reaction, indications for the existence of the higher energy member of the doublet were also found.

^{22}N was observed only in the double-step process. Its γ spectrum is rather clean; it contains only two γ rays at 183 and 834 keV which are in mutual coincidence, as demonstrated in Fig. 5.

The level schemes shown in Figs. 6, 7, 8, and 9 were constructed using the deduced $\gamma\gamma$-coincidence relations, the approximate intensities and the energy balance of the transitions.

In ^{19}N, on the basis of their coincidence relations, the 1141, 532, and 1494 keV γ rays are placed in cascade. Their order is determined by the relative intensities. The energy of the 1681(5) keV γ ray overlaps with the 1141(3)+532(2) keV sum energy within the error bars; thus, this line may correspond to a cross-over transition. As the 532 and 1141 keV γ rays have coincidence relations also with the 2347 keV transition, it is placed above the 1681 keV level establishing an excited state at 4023 keV. Based on the coincidence relations of the 1368 keV γ ray, it connects the level at 2511 keV to the first excited state. Since the 2132 keV transition does not seem to be in coincidence with any γ ray, it corresponds to a level decaying directly to the ground state. The weakly seen 2016 and 2507 keV transitions overlap with the sum of the 532+1494 and 1141+1368 keV transitions and are tentatively assigned as cross-over transitions from the 3170 and 2511 keV states, respectively. The energy of the excited states is determined with the fitting procedure of the RADWARE

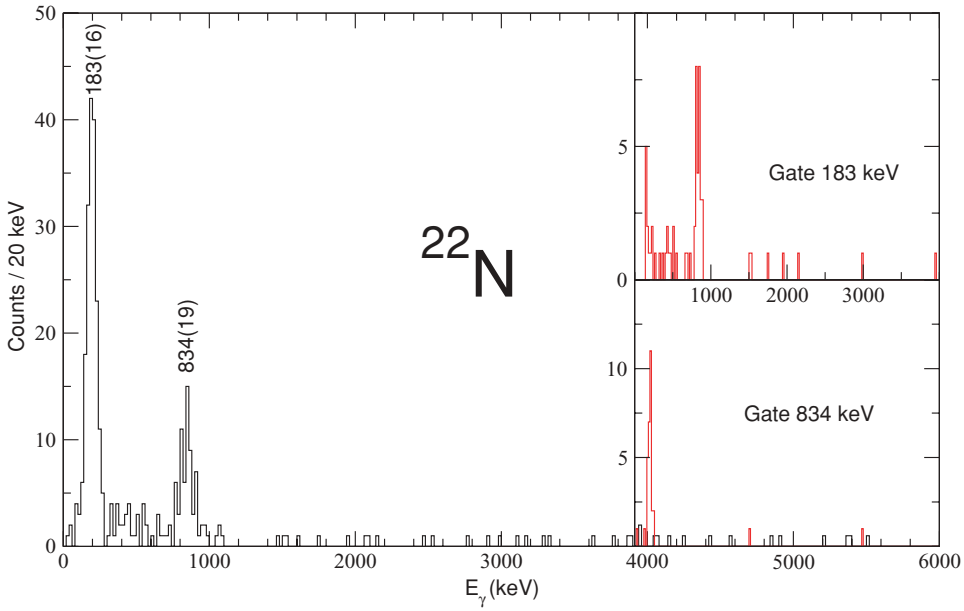

FIG. 5. (Color online) BaF_2 γ-ray spectrum of ^{22}N obtained in the double-step fragmentation reaction. Insets show BaF_2 coincidence spectra.

package [11] using the energy values and uncertainties of the corresponding feeding and deexciting γ rays. The two lowest energy excited states at 1143 and 1676 keV as well as the 2511 keV state are in good agreement with the energy of the excited states obtained in the multinucleon transfer reaction at 1110(20), 1650(20), and 2540(30) keV [7], respectively.

According to the $\gamma\gamma$-coincidence relations, the level scheme of ^{20}N consists of three branches of γ rays. The strongest, 843 keV transition is in coincidence with the 1052 and 2100 keV transitions, resulting in excited states at 1895 and 2943 keV. The 615 and 944 keV γ rays form another cascade establishing a state at 1559 keV. However, their order in the cascade is ambiguous, because their intensities are equivalent within the experimental errors. The 1336 keV transition, not seen in coincidence with any other transition, forms the third branch in the level scheme. It is worth mentioning that the neutron separation energy of ^{20}N is at 2161(52) keV [12]; thus, the highest energy state observed in the present case is well above the neutron threshold, similar to the case of ^{19}O [9].

In ^{21}N, the 1177 keV transition is the most intense one, and it is assigned to the decay of the first excited state to the ground state. The 1177 keV transition was found to be in coincidence with all the 1228, 1790, 2142, and 2438 keV γ rays. While the higher energy transitions of 2142 and 2438 keV see only the 1177 keV one in coincidence, the 1790 keV γ ray sees both the 1177 and 1228 keV ones. Thus, the 1228, 2142, and 2438 keV transitions decay parallel to each other to the first excited state, and the 1790 keV transition feeds the second excited state at 2405 keV. The 884 keV transition in coincidence with the 1177+1228 keV doublet fits the energy differences between the 3319 and 2405 keV states as well as that of the 4195 and 3319 keV ones and is placed there tentatively. Existence of a 1210 keV transition connecting the 3615 and 2405 keV states as well as that of a 2405 keV transition connecting the 2405 keV state with the ground state cannot be excluded. Actually, there is some indication of the existence of a coincidence relation between the 1790 and a ~2400 keV transition in the gate spectrum shown in the inset of Fig. 4. These transitions are tentatively included in the level scheme.

In ^{22}N, we have seen only two transitions, at 183 and 834 keV, which are in mutual coincidence, thus they are placed above each other forming a γ-ray cascade. The order of the transitions is determined by their intensities.

IV. DISCUSSION

A. Shell model interpretation of the experimental results

The structure of the heavy nitrogen isotopes has been calculated by use of the shell model in the full *psd* shell with the WBT interaction of Warburton and Brown [1], the *sd* part of which is the USD interaction [13].

Comparing the results of the calculation with the experimental data in Figs. 6 and 8, we see that the theoretical spectrum is expanded relative to the experimental one. A similar situation was observed also in the case of the heavy carbon nuclei [3], where a 25% decrease of the neutron-neutron interaction strength in the *sd* space was proposed. Applying the same procedure to the heavy nitrogen isotopes results in a compressed energy spectrum. Since the nitrogen nuclei are between the oxygen isotopes (where the USD interaction describes the excitation energies reasonably [9]) and the carbon ones (where a 25% decrease is needed), we applied a 12.5% decrease in the *sd* interaction strength, which resulted in a reasonable description (see the WBTM column in the

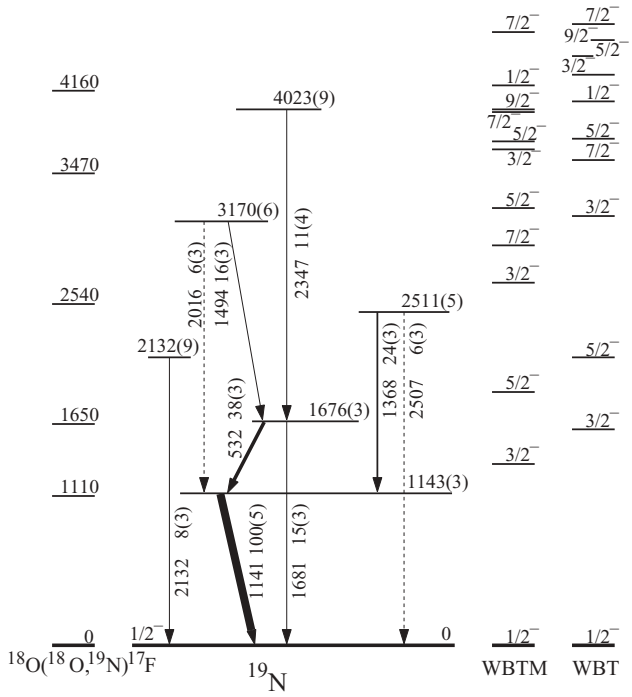

FIG. 6. Proposed level scheme of ^{19}N compared with the results of the multinucleon transfer experiment [7]. Along the transitions, their energies and relative intensities with uncertainties are given. The width of the arrows is proportional to the intensity of the γ rays. The results of the large-scale shell model calculations are shown along the right-hand side of the figure.

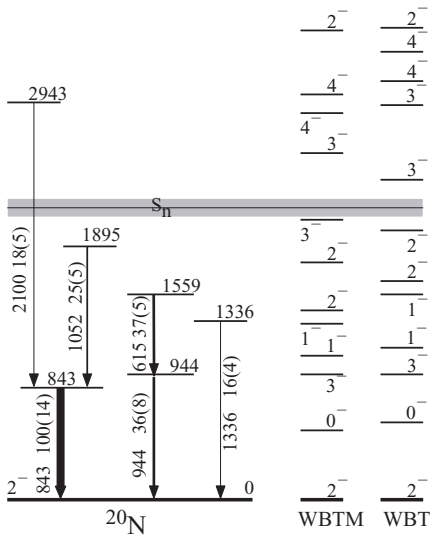

FIG. 7. Proposed level scheme of ^{20}N compared with shell model calculations based on the WBTM and WBT interactions.

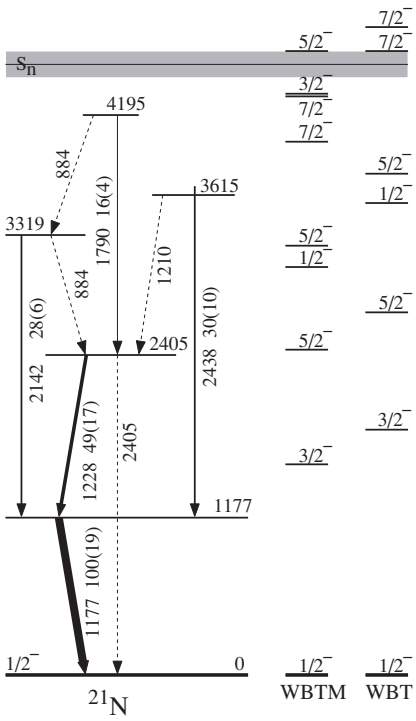

FIG. 8. Proposed level scheme of ^{21}N in comparison with the shell model calculations based on the WBT and the WBTM interactions.

figures). As an alternative solution, in Ref. [4] a 30% decrease of the monopole part of the *sd* interaction was proposed to describe the magnetic moment of ^{17}N. This results in an ~800 keV lowering of the excited states, which seems to be too much. Using half of this decrease, an ~400 keV lowering of the excited states would result in as satisfactory a description of the experimental energies as that obtained with the modified WBTM interaction.

Taking into account the calculated decay properties of the states, one can tentatively assign the experimental states to the theoretical ones. Using such an assignment, the first two excited states of ^{19}N arise from the coupling of the $p_{1/2}$ proton hole to the 2^+_1 state of the ^{20}O core. Comparing only the energies of the experimental and theoretical states, the 3170 keV state could correspond to the $7/2^-_1$ or the $5/2^-_2$ ones. If the 3170 keV state was the $5/2^-_2$ one, the transition connecting it to the $3/2^-_1$ state would be dominant. As the

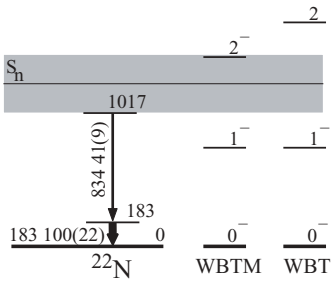

FIG. 9. Proposed level scheme of ^{22}N in comparison with the shell model calculations based on the WBT and the WBTM interactions.

1494 keV transition decaying to the likely $5/2^-_1$ state is much stronger, we propose that the 3170 keV state corresponds to the $7/2^-_1$ one. The 4023 keV state can be a good candidate for the $7/2^-_2$ theoretical state. The 2511 keV state strongly populates the 1143 keV state which is assigned to the $3/2^-_1$ theoretical one, while the 2132 keV state feeds the ground state. In ^{17}N, positive parity states have been observed at 1849 and 2526 keV [14] having analogous decay patterns to the 2132 and 2511 keV states in ^{19}N. Thus, these states may correspond to the intruder $1/2^+$ and $5/2^+$ states, respectively; although the decay pattern of the 2132 keV state allows for an assignment to the $3/2^-_2$ theoretical state, too.

In ^{21}N, the situation is rather similar to the ^{19}N case. The first two excited states arise from the coupling of the $p_{1/2}$ proton hole to the neutron 2^+ excitation of the ^{22}O core, while the 3319 and 4195 keV states are candidates for the $5/2^-_2$ and $7/2^-_1$ theoretical states arising from the coupling of the $p_{1/2}$ proton hole to the neutron 3^+ excitation. The 3615 keV state has no theoretical counterpart among the negative parity states and is again a candidate for being the intruder $5/2^+$ state.

For ^{20}N, the ground state is calculated to be 2^-. The calculated level density is much higher than in the odd nuclei, which makes the assignment of the theoretical states to the experimental ones more difficult. Nevertheless, the assignment of the 843 keV state to the 3^-_1 one, the 1895 keV state to the 3^-_2, and the 2943 keV state to the 4^-_1 theoretical one seems to be reasonable. The 4^- state lying above the neutron separation energy cannot be created by coupling of the $p_{1/2}$ proton hole to any of the low-lying neutron configurations, thus it is based on a core excited state. As a consequence, this state can decay by neutron emission to the ^{19}N ground state only in a two-step process, leaving room for a competing γ-decay channel. The 1336 keV state may correspond to either a 1^- or a 2^- theoretical configuration. The assignment of the 944/615 keV cascade is problematic. Considering the energy of these states, it would be a reasonable choice to assign them to a 1^-, 2^- doublet, but the 2^- states are expected to decay with a strong transition to the ground state, whereas such a transition is missing from the 1559 keV level. We cannot assign any of the 944 or 615 keV lines to the decay of the 0^- state calculated to be the first excited state either, because of its long 8 ns lifetime. The γ cascade in ^{22}N can be assigned to the decay of the 2^- state through the 1^- one to the 0^- ground state. The large difference between the calculated and experimental splitting of the $\pi p_{1/2}\nu s_{1/2}$ doublet may arise from the spatially extended nature of the neutron $s_{1/2}$ state [15]. Such an effect may also explain the problems in the assignment of the states of ^{20}N.

B. Stability of the shell closures

The existence of $N = 14, 16$ subshell closures has already been deduced from the analysis of the 1985 mass systematics [16] and confirmed later for a larger mass region [15]. The effect of these subshell closures is clearly shown in the ^{24,26}Ne isotopes, too, having relatively higher 2^+ energies and lower $E2$ transition probabilities than their neighbors. Recent transfer reaction studies of ^{23}O resulted in the determination of the energies of the $d_{3/2}$ [17] and $d_{5/2}$ [18] states relative to

the $s_{1/2}$ one, which made it possible to deduce the strength of the $N = 14$, 16 subshell closures at $Z = 8$.

The $N = 14$ subshell closure in the oxygen isotopes resulted in a sudden increase of the 2_1^+ state in ^{22}O [9], while such a sign of the $N = 14$ subshell closure is missing in the systematics of the heavy carbon nuclei [3]. Using the above tentative assignments of the experimental states, from the energies of the states coupling of the $p_{1/2}$ proton hole to the neutron 2^+ excitation, we can estimate an effective energy of the 2^+ excitation of the core in the extreme weak coupling model in the heavy nitrogen isotopes. For this purpose, the (2j+1) weighted average of the energies of the $3/2_1$ and $5/2_1$ states can be used following the center-of-gravity theorem first deduced by R. D. Lawson and J. L. Uretsky [19]. At $N = 10$ and 12, the effective 2^+ energies of 1687 and 1463 keV are slightly smaller than those of the carbon (1766 and 1585 keV) and oxygen (1982 and 1675 keV) isotopes with the same neutron number. At $N = 14$, there is a nearly 500 keV increase in the effective 2^+ energy, suggesting that the $N = 14$ subshell closure survives to some extent at $Z = 7$. Following the algorithm proposed in Ref. [9] to deduce the strength of the $N = 14$ shell closure in ^{22}O, we can deduce it as the weighted average of the energies of the effective 2^+ and 3^+ core excitations in ^{21}N. It results in 3.02 MeV, which is 1.2 MeV smaller than the value deduced for ^{22}O. Such a weakening of the $N = 14$ subshell closure is a result of the removal of a proton from the $p_{1/2}$ orbit. Using a linear extrapolation, if we remove both $p_{1/2}$ protons, the $N = 14$ shell gap gets only 1.82 MeV, which may explain why no signs of the $N = 14$ subshell closure are visible in ^{20}C.

The transitional nature of the nitrogen isotopes between the oxygen and carbon ones having the same neutron number is supported also by the calculated $B(E2)$ values. Using $e_p = 1.5\,e$ and $e_n = 0.5\,e$ effective charges, the shell model gives 29 and 24 e^2 fm^4 for the $B(E2; 0^+ \rightarrow 2^+)$ transition probability for ^{20}O and ^{22}O, respectively, which are in accordance with the experimental values: 28(2) [20] and 21(8) [21] e^2 fm^4. According to the weak coupling approximation [22], the sum of the $E2$ strengths from the ground state to the $3/2^-$ and $5/2^-$ states in the nitrogen isotopes should equal that of the $B(E2; 0^+ \rightarrow 2^+)$ strength in their appropriate oxygen cores. The shell model calculations give a 48 e^2 fm^4 sum strength for the ^{19}N, and a 54 e^2 fm^4 one for ^{21}N, which are about twice the oxygen values and lie about half way between the neighboring oxygen and carbon $B(E2; 0^+ \rightarrow 2^+)$ values. This fact shows that the core structure of the nitrogen isotopes is more soft than that of the singly closed shell oxygen isotopes.

In ^{15,17}N, the energy of the positive parity intruder states is known, and we have a candidate for the $5/2^+$ state in ^{19,21}N, too. Their energies are 5270, 2526, 2511, and 3615 keV in ^{15}N [23], ^{17}N [14], ^{19}N, and ^{21}N, respectively. Lowering of the energy of the intruder states in ^{17,19}N can be associated with the binding energy gain due to deformation. On the other hand, considering that ^{15}N and ^{21}N are neutron closed shell nuclei, the change of the energy of the intruder configuration can be assigned to the change of the shell gap. Thus, adding six $d_{5/2}$ neutrons to the ^{15}N nucleus, the $Z = 8$ shell gap gets weaker by 1645 keV. This estimate is in agreement with the previous observation, according to which the $Z = 8$ shell gap gets weaker by 1.5(3) MeV while going from ^{16}O to ^{22}O [5]. In the shell model calculation, the $5/2^+$ state is at 4.889 keV in ^{21}N, at a slightly lower energy than observed in ^{15}N. This suggests that the WBT interaction does not account fully for the weakening of the $Z = 8$ shell closure. Indeed, also in ^{19}N, the energy of the intruder states is overestimated by 1.2–1.4 MeV. It is worth mentioning that the energy of the lowest lying intruder configuration in ^{20}N is calculated at 1.79 MeV. The presence of an intruder configuration at low energy may be another reason for the difficulties in the assignment of all the ^{20}N states to negative parity configurations.

V. SUMMARY

The structure of the neutron-rich $^{19-22}$N nuclei has been investigated by in-beam γ-ray spectroscopy of the fragmentation of stable and radioactive beams. From particle-γ and particle-$\gamma\gamma$ coincidence relations, γ rays have been assigned to the decay of the excited states of the nuclei investigated, and level schemes have been proposed for the first time. The experimental states could be assigned tentatively to the theoretical ones in the odd-mass nuclei ^{19,21}N from a comparison with shell model calculations performed in the *psd* model space. From the mass dependence of the effective 2^+ energy of the neutron core deduced in the extreme weak coupling model from the tentatively assigned states in the nitrogen isotopic chain, a partial survival of the $N = 14$ subshell closure was deduced, the strength of which has been estimated at 3.02 MeV. A 1.6 MeV decrease of the $Z = 8$ shell closure was also deduced as a result of adding six $d_{5/2}$ neutrons to ^{15}N from the change of the energy of the proposed intruder proton $d_{5/2}$ configuration. A discrepancy between the calculated and measured energies of the excited states was observed using the WBT interaction, which suggests that the USD part of the WBT interaction is about 12.5% stronger than required. This reduction is half the value observed in heavy carbon nuclei [3], as well as the value proposed to account for the correlations needed to interpret the magnetic moment of ^{17}N [4].

ACKNOWLEDGMENTS

This work has been supported by the European Community through the Eurons Contract RII3-CT-2004-506065, by OTKA T46901, K68801, NSF PHY-0244453, and by Czech Republic GA No. 202/04/0791 grants.

[1] E. K. Warburton and B. A. Brown, Phys. Rev. C **46**, 923 (1992).
[2] M. Stanoiu, M. Belleguic, Zs. Dombrádi, D. Sohler, F. Azaiez, B. A. Brown, M. J. Lopez-Jimenez, M. G. Saint-Laurent, O. Sorlin, Yu.-E. Penionzhkevich, N. L. Achouri, J. C. Angelique, C. Borcea, C. Bourgeois, J. M. Daugas, F. De Oliveira-Santos, Z. Dlouhy, C. Donzaud, J. Duprat, S. Grévy,

D. Guillemaud-Mueller, S. Leenhardt, M. Lewitowicz, S. M. Lukyanov, W. Mittig, M. G. Porquet, F. Pougheon, P. Roussel-Chomaz, H. Savajols, Y. Sobolev, C. Stodel, and J. Timár, Eur. Phys. J. A **22**, 5 (2004).

[3] M. Stanoiu, F. Azaiez, F. Becker, M. Belleguic, C. Borcea, C. Bourgeois, B. A. Brown, Z. Dlouhy, Z. Dombrádi, Z. Fülöp, H. Grawe, S. Grévy, F. Ibrahim, A. Kerek, A. Krasznahorkay, M. Lewitowicz, S. Lukyanov, H. van der Marel, P. Mayet, J. Mrazek, S. Mandal, D. Guillemaud-Mueller, F. Negoita, Y. E. Penionzhkevich, Z. Podolyák, P. Roussel-Chomaz, M. G. Saint Laurent, H. Savajols, O. Sorlin, G. Sletten, D. Sohler, J. Timár, C. Timis, and A. Yamamoto, Eur. Phys. J. A **20**, 95 (2004).

[4] H. Ueno, K. Asahi, H. Izumi, K. Nagata, H. Ogawa, A. Yoshimi, H. Sato, M. Adachi, Y. Hori, K. Mochinaga, H. Okuno, N. Aoi, M. Ishihara, A. Yoshida, G. Liu, T. Kubo, N. Fukunishi, T. Shimoda, H. Miyatake, M. Sasaki, T. Shirakura, N. Takahashi, S. Mitsuoka, and W.-D. Schmidt-Ott, Phys. Rev. C **53**, 2142 (1996).

[5] M. Wiedeking, S. L. Tabor, J. Pavan, A. Volya, A. L. Aguilar, I. J. Calderin, D. B. Campbell, W. T. Cluff, E. Diffenderfer, J. Fridmann, C. R. Hoffman, K. W. Kemper, S. Lee, M. A. Riley, B. T. Roeder, C. Teal, V. Tripathi, and I. Wiedenhover, Phys. Rev. Lett. **94**, 132501 (2005).

[6] F. Naulin, C. D. Detraz, M. Roy-Stephan, M. Bernas, J. de Boer, D. Guillemad, M. Langevin, F. Pugheon, and P. Roussel, J. Physique Lett. **43**, 29 (1982).

[7] W. N. Catford, L. K. Fifield, N. A. Orr, and C. L. Woods, Nucl. Phys. **A503**, 263 (1989).

[8] E. Sauvan, F. Carstoiua, N. A. Orr, J. C. Angelique, W. N. Catford, N. M. Clark, M. Mac Cormick, N. Curtis, M. Freer, S. Grévy, C. Le Brun, M. Lewitowicz, E. Liégard, F. M. Marques, P. Roussel-Chomaz, M. G. Saint Laurent, M. Shawcross, and J. S. Winfield, Phys. Lett. **B491**, 1 (2000).

[9] M. Stanoiu, F. Azaiez, Zs. Dombrádi, O. Sorlin, B. A. Brown, M. Belleguic, D. Sohler, M. G. Saint Laurent, J. Lopez-Jimenez, Y. E. Penionzhkevich, G. Sletten, N. L. Achouri, J. C. Anglique, F. Becker, C. Borcea, C. Bourgeois, A. Bracco, J. M. Daugas, Z. Dlouhy, C. Donzaud, J. Duprat, Zs. Fülöp, D. Guillemaud-Mueller, S. Grévy, F. Ibrahim, A. Kerek, A. Krasznahorkay, M. Lewitowicz, S. Leenhardt, S. Lukyanov, P. Mayet, S. Mandal, H. van der Marel, W. Mittig, J. Mrazek, F. Negoita, F. De Oliveira-Santos, Zs. Podolyák, F. Pougheon, M. G. Porquet, P. Roussel-Chomaz, H. Savajols, Y. Sobolev, C. Stodel, J. Timár, and A. Yamamoto, Phys. Rev. C **69**, 034312 (2004).

[10] M. Belleguic, F. Azaiez, Zs. Dombrádi, M. J. Lopez-Jimenez, T. Otsuka, M. G. Saint-Laurent, D. Sohler, O. Sorlin, M. Stanoiu, Y. Utsuno, Yu.-E. Penionzhkevich, N. L. Achouri, J. C. Angelique, C. Borcea, C. Bourgeois, J. M. Daugas, F. De Oliveira-Santos, Z. Dlouhy, C. Donzaud, J. Duprat, Z. Elekes, S. Grévy, D. Guillemaud-Mueller, S. Leenhardt, M. Lewitowicz, S. M. Lukyanov, W. Mittig, M. G. Porquet, F. Pougheon, P. Roussel-Chomaz, H. Savajols, Y. Sobolev, C. Stodel, and J. Timár, Phys. Rev. C **72**, 054316 (2005).

[11] D. C. Radford, Nucl. Instrum. Methods A **361**, 297 (1995).

[12] G. Audi, O. Bersillon, J. Blachot, and A. H. Wapstra, Nucl. Phys. **A624**, 1 (1997).

[13] B. H. Wildenthal, Prog. Part. Nucl. Phys. **11**, 5 (1984).

[14] D. R. Tilley, H. R. Weller, and C. M. Cheves, Nucl. Phys. **A564**, 1 (1993).

[15] A. Ozawa, T. Kobayashi, T. Suzuki, K. Yoshida, and I. Tanihata, Phys. Rev. Lett. **84**, 5493 (2000).

[16] A. Abzouzi and M. S. Antony, Nuovo Cimento **97**, 753 (1987).

[17] Z. Elekes, Zs. Dombrádi, N. Aoi, S. Bishop, Zs. Fülöp, J. Gibelin, T. Gomi, Y. Hashimoto, N. Imai, N. Iwasa, H. Iwasaki, G. Kalinka, Y. Kondo, A. A. Korsheninnikov, K. Kurita, M. Kurokawa, N. Matsui, T. Motobayashi, T. Nakamura, T. Nakao, E. Yu. Nikolskii, T. K. Ohnishi, T. Okumura, S. Ota, A. Perera, A. Saito, H. Sakurai, Y. Satou, D. Sohler, T. Sumikama, D. Suzuki, M. Suzuki, H. Takeda, S. Takeuchi, Y. Togano, and Y. Yanagisawa, Phys. Rev. Lett. **98**, 102502 (2007).

[18] A. Schiller, N. Frank, T. Baumann, D. Bazin, B. A. Brown, J. Brown, P. A. DeYoung, J. E. Finck, A. Gade, J. Hinnefeld, R. Howes, J.-L. Lecouey, B. Luther, W. A. Peters, H. Scheit, M. Thoennessen, and J. A. Tostevin, Phys. Rev. Lett. **99**, 112501 (2007).

[19] R. D. Lawson and J. L. Uretsky, Phys. Rev. **108**, 1300 (1957).

[20] S. Raman, At. Data Nucl. Data Tables **36**, 1 (1987).

[21] P. G. Thirolf, B. V. Pritychenko, B. A. Brown, P. D. Cottle, M. Chromik, T. Glasmacher, G. Hackman, R. W. Ibbotson, K. W. Kemper, T. Otsuka, L. A. Riley, and H. Scheit, Phys. Lett. **B485**, 16 (2000).

[22] K. Alder, A. Bohr, T. Huus, B. Mottelson, and A. Winther, Rev. Mod. Phys. **28**, 432 (1956).

[23] F. Ajzenberg-Selove, Nucl. Phys. **A523**, 1 (1991).